

How initial and boundary conditions affect protoplanetary migration in a turbulent sub-Keplerian accretion disc: 2D SPH simulations

V. Costa^{1*}, V. Pirronello¹, G. Belvedere², A. Del Popolo², D. Molteni³, G. Lanzafame⁴

¹*Dipartimento di Metodologie Chimiche e Fisiche per l'Ingegneria, Università di Catania, Viale A. Doria 6, I-95125, Catania, Italy*

²*Dipartimento di Fisica e Astronomia, Università di Catania, Sezione Astrofisica, Via Santa Sofia 78, I-95125, Catania, Italy*

³*Dipartimento di Fisica e Tecnologie Relative, Università di Palermo, Viale delle Scienze, I-90128, Palermo, Italy*

⁴*Osservatorio Astrofisico di Catania, Istituto Nazionale di Astrofisica, Via S. Sofia 78, I-95123, Catania, Italy*

ABSTRACT

Current theories on planetary formation establish that giant planet formation should be contextual to their quick migration towards the central star due to the protoplanets-disc interactions on a timescale of the order of 10^5 years, for objects of nearly 10 terrestrial masses. Such a timescale should be smaller by an order of magnitude than that of gas accretion onto the protoplanet during the hierarchical growing-up of protoplanets by collisions with other minor objects. These arguments have recently been analysed using N-body and/or fluid-dynamics codes or a mixing of them. In this work, inviscid 2D simulations are performed, using the SPH method, to study the migration of one protoplanet, to evaluate the effectiveness of the accretion disc in the protoplanet dragging towards the central star, as a function of the mass of the planet itself, of disc tangential kinematics and of the presence of a planet “pseudo-atmosphere”. To this purpose, the SPH scheme is considered suitable to study the roles of turbulence, kinematic and boundary conditions, due to its intrinsic advective turbulence, especially in 2D and in 3D codes. Simulations are performed both in disc sub-Keplerian and in Keplerian kinematic conditions. Our results show migration times of a few orbital periods for Earth-like planets in sub-Keplerian conditions, while for Jupiter-like planets estimates give that about 10^4 orbital periods are needed to half the orbital size. The planet pseudo-atmosphere seems to prolong migration times in some cases. Moreover timescales of planet migration are strongly dependent on the relative position of the planet with respect to the shock region near the centrifugal barrier of the disc flow.

Key words: planetary systems: formation – planetary systems: protoplanetary discs

1 INTRODUCTION

Currently, nearly 300 extra-solar planets have been detected (<http://www.exoplanets.eu/>), and most of them are massive (Jupiter-like) planets with small (fractions of AU) semi-major axes (see Perryman (2000) and Udry & Santos (2007) for a review on detection methods and on the main properties of exo-planets). Theoretical models for the formation of planetary systems are then mostly based on the crucial role of an accretion disc around a forming young star, where the disc provides both the material for the forming planets and the interactions responsible for the migration of the protoplanets towards the central star. The need for proto-

planetary migration comes from the difficulty of an “in situ” formation in such close to the star positions, so that the detailed understanding of migration mechanisms appears mandatory in order to build self-consistent models for planetary systems formation. Some analytic studies on the matter (Goldreich & Tremaine 1979, 1980; Lin & Papaloizou 1984, 1986a,b; Ward 1997) suggest that gravitational torques due to resonant non-axisymmetric structures could act to transfer angular momentum between the protoplanets and the disc (for a discussion of other alternative migration models see Del Popolo et al. (2005) and references therein). The gravitational disturbance exerted by the protoplanet on the disc produces spiral density waves which break the axial symmetry of the disc structure. Perturbation theory allows an estimate of the net torque that this perturbed disc ex-

* E-mail: vcosta@oact.inaf.it

erts back onto the planet at “Lindblad resonance sites” (Goldreich & Tremaine 1980; Ward 1997). This disc-planet interaction induces also a repulsion of material on either side of the protoplanet’s orbit, with a possible formation of a density gap, depending on the interaction strength. Two main migration types are then distinguished: *type I* (Tanaka et al. 2002), when an Earth-like planet, not capable of opening a density gap in the disc is embedded in the disc structure. In this case the migration rate should be proportional to the protoplanet mass; *type II* when a massive protoplanet, capable of opening and maintaining a density gap, remains trapped in this gap. In this case migration is due to the viscosity dominated evolution of the disc. In both cases it is possible that the lifetime of migration is shorter than the lifetimes of planet formation or disc dissolution, causing the collapse of the planet toward the star. Accurate numerical simulations are necessary to better understand the matter (Papaloizou et al. 2006). The main aim of this work is to study the role of initial and boundary conditions on planetary migration as a consequence of planet-disc dynamic interaction during the initial formation phases of stellar systems. Several papers devoted to this theme, according to various fluid-dynamics schemes (Artymowicz 2004; D’Angelo et al. 2002, 2003, 2006; Kley 2000; Papaloizou et al. 2006; Schäfer et al. 2004), showed that this mechanism should be very effective for the protoplanet dragging toward the central protostar in characteristic time-scales of the order of 10^5 years. However, these studies assume that the accretion disc is basically Keplerian and pressure forces are often neglected among the protostar-disc interactions. Therefore, the roles of sub-Keplerian flows still needs to be investigated.

The possibility to find sub-Keplerian flows in the formation of protoplanetary accretion discs is here taken into account (see section 2.2 for details on exact initial conditions). It should be noted that in Keplerian models, the Keplerian distribution of disc gas velocity is usually assumed as a hypothesis (Cresswell & Nelson 2006; de Val-Borro et al. 2006; Kley 2000; Schäfer et al. 2004; Terquem et al. 2000). However, even if an initially infalling protostar cloud, due to its intrinsic angular momentum, will form a disc-like structure, there is no guarantee that the formed disc will have a permanent purely Keplerian velocity distribution. An infalling gas component (sub-Keplerian flow) could continue to have a role in the evolution of the a disc during a protoplanet formation phase (Sollins & Ho 2005; Ulrich 1976). Besides, some authors already treated some slightly sub-Keplerian gas flows in their models, even if limited to a small correction due to the contribution of pressure gradients (Paardekooper & Mellema 2004). Moreover, even if a hydrodynamical simulation is started with a disc structure with a purely Keplerian velocity distribution, this velocity profile can only survive for a system of “not interacting” particles. In the presence of significant pressure forces and/or viscosity, gas particle collisions and transport processes will change the initial configuration (see section 4 for a numerical test of this effect), so that the production of sub-Keplerian flows is real effect. Complex cloud fragmentation of star forming regions and gas acceleration with complex fluid dynamics effects is also provided, in proper circumstances, by shock-cloud interactions, as discussed by Xu & Stone (1995).

In this paper we produce results with several Cartesian 2D SPH sub-Keplerian disc models, also considering the role of the presence of a planet gaseous atmosphere interacting with the gaseous disc, paying attention to differences in planetary migration both for one Jovian and for one Terrestrial planet. Models of Jovian or Terrestrial planets, interacting with an initial Keplerian accretion disc, are also produced for a strict comparison. The coming out of shock fronts and complex structures, both steady and progressive in sub-Keplerian turbulent accretion flows in AGN, was described in Chakrabarti & Molteni (1993), Molteni et al. (1994), Lanzafame et al. (1998), as well as pulsed or periodic outflows in Lanzafame et al. (2008) as a consequence of collisional interactions in the disc surrounding the central accreting object in axial symmetry. In such environments (AGN or equivalently protostellar systems), the potential importance of the centrifugal barrier in developing outflow structures in turbulent collisional fluid-dynamics, was successfully described in those papers. This implies that the possibility of a slower dragging toward the central star cannot be excluded in principle. Therefore, as a secondary aim, the purpose of the paper is the methodical search for those initial and boundary conditions determining results showing how Jovian and Terrestrial protoplanets could stay in orbits surrounding the central stars at distances of the order of that of Venus or Mercury.

In section 2 we discuss the initial and boundary conditions characterising our models. In sec. 3 we describe our results, and we discuss them in section 4.

2 MODELS FEATURES AND BOUNDARY CONDITIONS

2.1 Models

The simulations presented in this work are based on a two-dimensional model which makes use of the Smoothed Particle Hydrodynamics (SPH) numerical method (Monaghan 1992). The choice of using the SPH method is funded on the grounds of its Lagrangian nature and its ability to easily tackle hydrodynamic problems with free surfaces. The ability of many different numerical schemes, both grid-based and Lagrangian, to correctly describe planet-gas interactions was tested by de Val-Borro et al. (2006), showing that SPH is not significantly less performant than other methods. Given the lack of a wide range of case studies on the matter in SPH, we believe that our work could give an interesting contribution to improve the basic knowledge on disc-protoplanet interaction.

The code does not contain a specific radiation treatment, but the used equation of state: $P = (\gamma - 1)\rho u$, where u is the thermal energy per unit mass, includes the polytropic index γ , which can be adjusted to values lower than $5/3$ if radiation, partial molecular dissociation or partial ionisation effects are present, giving the overall effect of a higher compressibility to the gas. Current calculations are performed with the simple choice of $\gamma = 5/3$, but we intend to further investigate this matter in a future work.

The model is built in Cartesian coordinates with dimensionless quantities. Reference physical units are:

- the initial stellar mass M_0 ;

- the stellar radius R_0 ;
- the Keplerian period of an orbit of radius R_0 around a star of mass M_0 , $T_0 = \frac{2\pi}{\sqrt{GM_0}} R_0^{3/2}$

With these choices, the following units can be used to transform our numerical results in physical quantities:

- velocity: $v_0 = \frac{1}{2\pi} \sqrt{\frac{GM_0}{R_0}}$
- specific angular momentum: $j_0 = \frac{1}{2\pi} \sqrt{GM_0 R_0}$
- energy per unit mass: $u_0 = \frac{1}{4\pi^2} \frac{GM_0}{R_0}$
- surface density: $\sigma_0 = \frac{M_0}{R_0^2}$

The initial conditions used to build the accretion disc are axially symmetric. The accretion disc is in fact created through the injection of particles at point-like positions (injectors) along circles concentric with the central star. Particles have initial tangential velocities set by choosing a value for the angular momentum per unit mass j . At some point, the accretion disc reaches a “nearly” steady state population of particles (time averaged since some variation of the number of particles and of the density distributions are actually observed during our simulations, due to the highly turbulent nature of our calculated flows) with $3 \times 10^5 - 5 \times 10^5$ particles, depending on the model, when using a smoothing length (spatial resolution parameter of the SPH method) $h = 0.3$. At this stage, the planet is inserted and the model is evolved. We included the following interactions in our models:

- (i) gravitational interaction between gas particles and central star;
- (ii) gravitational interaction between planet and star;
- (iii) gravitational interaction between particles and planet;
- (iv) gas pressure between neighbouring gas particles;
- (v) artificial viscosity (pressure contribution) between gas particles;
- (vi) gas particle capture by the planet (conservation of momentum is used to correct the planet speed before removing the particle) when gas particles approach the planet area (planet-particle distance less than $2h$).

Additionally, in some of our models, an SPH particle is given the planet position and velocity. This allows an interaction between the protoplanet and the gas particles, with consequent momentum transfer through pressure forces instead of using only inelastic particle captures. This approach is hereafter indicated as adding a “pseudo-atmosphere” to the protoplanet.

No self-gravitation is included in the gas for computational reasons, and this is not believed to negatively affect our computations since the disc total mass is $10^{-11} \times$ the number of particles, which for $\sim 10^5$ particles means 10^{-6} (in units of the central star mass M_0), so that the dominating gravitational force is still that of the central star. Reported values for disc masses are in the range $10^{-3} - 10^{-1} M_\odot$ on the grounds of observational constraints from T-Tauri stars (Hartmann 2000; Terquem et al. 2000), but this value is usually distributed over a disc with a radius of $100 - 1000 AU$. In order to compare this to the structure of our simulated disc, given the dimensionless nature of our simulation, we need to choose some physical reference units. If $1 M_\odot$ and $2-3 R_\odot$ are taken for a typical T-Tauri star (Bertout 1989), the disc has a dimension of about $\sim 2 AU$. Therefore our

simulations cover only the central part of a typical T-Tauri accretion disc, and the mass included in the simulation is in agreement with observational constraints.

Most accretion disc models in literature include viscosity, according to the disc model of Shakura & Sunyaev (1973). Even today, it is hard to find a self-consistent way to give a correct value for the α viscosity parameter. We choose instead to not include physical viscous terms in the equations of our models, because we are here focused on the protoplanet migration mechanism based on gravitational and pressure forces and momentum transfer through gas particle captures, rather than to viscosity driven migration. Moreover, the absence of physical viscosity enhances the turbulent nature of our simulation, allowing us to correctly describe some effects due to turbulence like the development of non-axisymmetric structures in the disc (induced also by the presence of the protoplanet). Turbulence might also produce stronger shock fronts when infalling gas particles hit the centrifugal barrier.

There are plans to include physical viscosity in a future work, in order to better explore the viscosity driven migrations (like in type II migration models) and viscosity contribution in general.

2.2 Initial conditions

Three choices are made here for the angular momentum per unit mass j : 18, 36, 54, for particles injected at a radial distance of 130. All the three choices give a sub-Keplerian feature to the velocity distribution of the accretion disc (particles injected at a radial distance of 130 would have Keplerian velocity with $j \sim 70$), so that injected particles start decreasing their distance to the centre, until they “hit” the centrifugal barrier. These choices are considered in the framework of a parametric study, to test the effect of a wide range of possible conditions, from “extreme” ($j = 18$) to “weak” ($j = 54$) sub-Keplerian. The mass of the particles is set to 10^{-11} (in units of M_0), which means that the total mass of the disc can be about $10^{-6} - 10^{-5}$. Calculations are performed with two masses for the planet: 10^{-7} (Earth-like planet) and 10^{-3} (Jupiter-like planet). The computational domain is circular, extended in the xy plane with a radius of 150 (the star is located in the “origin”), and the planet is located inside the disc plane, with the initial position at $X_p = 100$ and $Y_p = 0$, and an initial zero eccentricity.

The azimuthally averaged density profiles of the sub-Keplerian accretion discs, just before planet insertion, are plotted in figure 1 for the three cases ($j = 18, 36, 54$). A Density peak is present near the centrifugal barrier in each case.

As far as the disc material accretion rate onto the central star, if $1 M_\odot$ and $2-3 R_\odot$ are taken for a typical T-Tauri star (Bertout 1989), we obtain for the three cases values of 2×10^{-6} , 6×10^{-7} , $3 \times 10^{-7} M_\odot/\text{year}$ with oscillations of about 30%, 80%, 100%. These values are in agreement with estimated accretion rates for T-Tauri stars (Gullbring et al. 1998; Hartigan, Edwards & Ghandour 1995).

In order to compare some of our results with more traditional models, some computations (two with an Earth-like planet and two with a Jupiter-like planet) are built using an initial exactly Keplerian distribution of gas particle velocities, with an initial uniform density over the entire disc area.

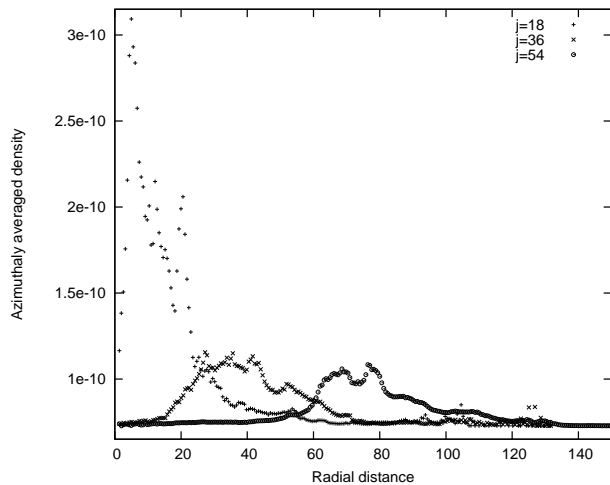


Figure 1. Azimuthally averaged density profiles of the sub-Keplerian accretion discs, just before planet insertion, for $j = 18, 36, 54$.

Label	j	M_p	pseudo-atmosphere
18a	18.0	10^{-3}	no
18b	18.0	10^{-3}	yes
18c	18.0	10^{-7}	no
18d	18.0	10^{-7}	yes
36a	36.0	10^{-3}	no
36b	36.0	10^{-3}	yes
36c	36.0	10^{-7}	no
36d	36.0	10^{-7}	yes
54a	54.0	10^{-3}	no
54b	54.0	10^{-3}	yes
54c	54.0	10^{-7}	no
54d	54.0	10^{-7}	yes
kepl_a	71.6	10^{-3}	no
kepl_b	71.6	10^{-3}	yes
kepl_c	71.6	10^{-7}	no
kepl_d	71.6	10^{-7}	yes

Table 1. List of computed models, with their identifying labels (first column). The second column gives the specific angular momentum of injected gas particles, the third column gives the initial mass of the protoplanet and the fourth column indicates the eventual presence of the pseudo-atmosphere on the protoplanet.

For simplicity, we will refer to these models as “Keplerian”, even if the velocity distribution of the gas particles cannot remain exactly Keplerian during the simulation, due to the pressure forces within the gas and to the interactions between the planet and the accretion disc. These models will be used to test the eventual formation of a gap near the protoplanet location, and to compare some classical views on the subject (Ward 1997) with our results obtained with an inviscid model.

A summary of the distinguishing features of our models is given in table 1 together with identifying labels. In the table, M_p is the mass of the planet in units of the central star mass, and “pseudo-atmosphere” indicates the eventual presence of a gas SPH particle associated with the planet.

3 RESULTS

The turbulent nature of our disc models is evidenced by the high value of the Reynolds number, evaluated by using the artificial viscosity coefficient $\nu_{num} = c_s h$ (Molteni et al. 1991), especially at the disc outer edge, where we have values of about 1200, 2400, 3600 for $j = 18, 36, 54$ respectively. Instead, in the innermost regions, where the disc gas temperature is higher, we still evaluate Re values of about $300 \div 1000$.

Figures 2-9 show the evolution of the orbital parameters for all models. The semi-major axis a as a function of time is shown in the top rectangle of each figure; the angular momentum of the protoplanet per unit mass l_z , the coordinate x and the eccentricity e are shown in the following rectangles, respectively. The coordinate x is plotted to show the orbital phase, which allow us to count protoplanet orbits. Each figure includes the results from two models, with (models with labels “b” and “d”) and without (models “a” and “c”) the pseudo-atmosphere gas particle for the planet. The main feature that emerges from the sub-Keplerian models is a downward migration of the protoplanet, the speed of which being strongly dependent on the planet mass. Earth-like planets migrate in a few orbits, especially in the $j = 18$ case, while for the Jupiter-like planets, an extrapolation of our results (which are limited to 20-30 orbits), suggests that a few thousands orbits are necessary to move the planets towards the central star.

Of course, the above suggested extrapolation would require a linear behaviour of the semi-major axis (or the specific angular momentum of the planet) with respect to time. But the results obtained for the less massive planet suggest that the migration rate asymptotically decreases for all the three values of the sub-Keplerian angular momentum of the injected particles. All the sub-Keplerian models with the Jovian planet lack the “classical” gap opening around the planet. This is not believed to be a problem as the type II migration mechanism, with the planet blocked inside the induced density gap, was developed in the framework of a Keplerian gas distribution in the accretion disc and within a viscosity based fluid model. Therefore the migration mechanism suggested within our model cannot be directly associated to the classical type I - type II distinction.

For the Keplerian models, fig. 8 shows that the Jupiter-like planet migration slowly proceeds outwards, despite the development of density gap soon after the introduction of the planet in the initially totally Keplerian gas distribution (fig. 16), while the Earth-like planet (fig. 9) migrates downward, with a slower rate when compared to that of sub-Keplerian discs. We have in fact 0.6% variation in a in about 30 orbits, while, with the same number of orbits, the sub-Keplerian discs show a $\sim 90\%$; 80% ; 50% decrease of the planet semi-major axis, for $j_z = 18$; 36 ; 54 respectively. As far as the influence of the pseudo-atmosphere is concerned, the difference between the results obtained with and without this model structure is of the order of $\sim 10^{-2}\%$ with the Jovian protoplanet and of $\sim 1 - 4\%$ with the Terrestrial protoplanet. In most cases we have an initial faster migration rate with the pseudo-atmosphere, but the situation is inverted after a few protoplanet’s orbits. This is clearer in models with a Terrestrial protoplanet for which

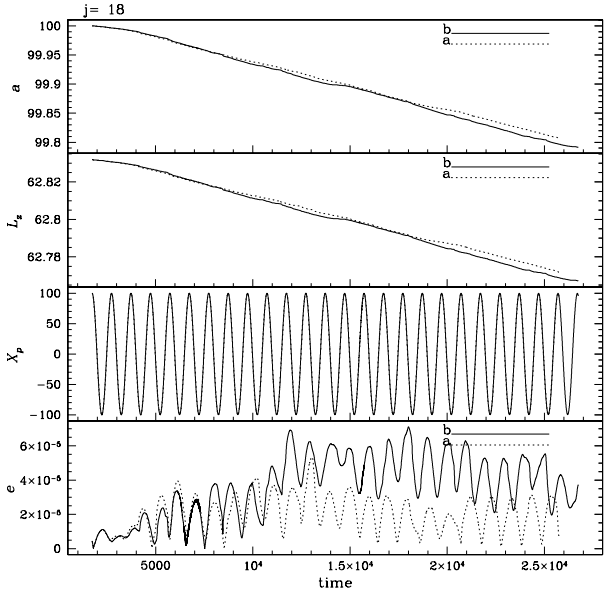


Figure 2. Orbital parameters evolution for models 18a and 18b. The semi-major axis a , the specific angular momentum l_z , the x coordinate of the protoplanet and the eccentricity e are reported, as a function of time. The dotted and continuum graphs are for the two reported data sets, with and without the protoplanet pseudo-atmosphere.

migration rate is much faster in all models. A significant difference is registered between the 54c and 54d models, where a $\sim 10 - 15\%$ difference is obtained in the semi-major axis a in advanced migration phases. The model without the pseudo-atmosphere (54c) suffers the fastest migration rate at some point.

In order to draw a semi-analytic behaviour in the orbital parameters evolution of the planets in our models, best-fits have been computed for the specific angular momentum j (figures 10-13) to have an estimate of the time derivatives and decrease lifetime of the angular momentum. Two kind of fits have been used: linear and exponential, according to the following schemes:

$$j_z = a * \exp(b \cdot t) + c * \exp(d \cdot t) + e \quad (1)$$

$$j_z = at + b \quad (2)$$

Tables 2 and 3 report the best-fit parameters obtained for the various models.

In table 2 the last two columns give the inverse values of the parameters b and d , and they have been dimensioned in years by choosing $1 M_\odot$ and $2 R_\odot$ as reference units. Of the two time-scales estimated in this way, the most important is the one with the corresponding highest “multiplying factor for the exponential” (a or c). For Jupiter-like planets these estimates must be taken with some care, as the simulations did not go enough far in time to have a clear path of the migration process, so that migration timeline of these models could be different than what expected from extrapolations.

In table 3 the 4th column gives a dimensionless migration time, evaluated as $l_z/l_{z,0}$, and the last column gives the same

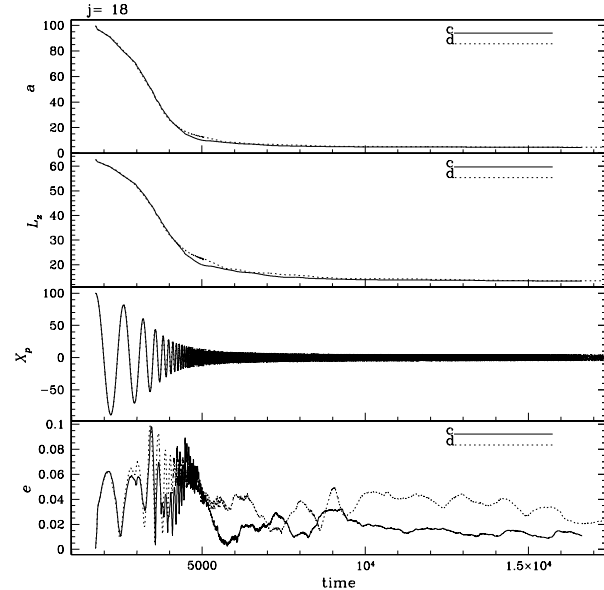


Figure 3. Orbital parameters evolution for models 18c and 18d. See fig. 2 caption for description.

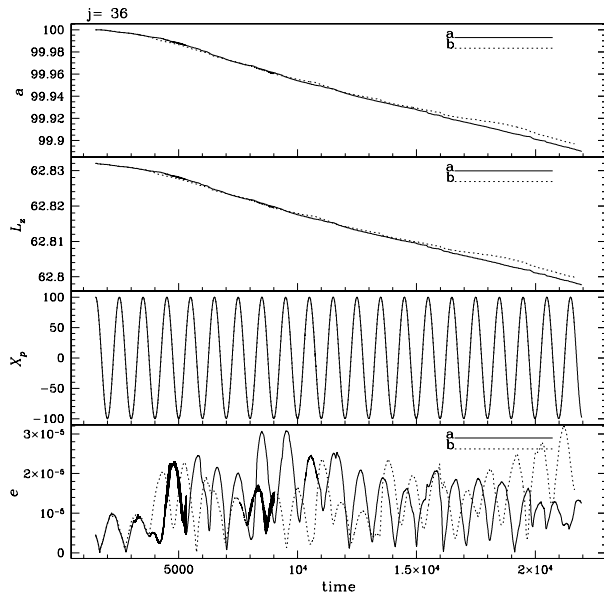


Figure 4. Orbital parameters evolution for models 36a and 36b. See fig. 2 caption for description.

time converted in years by choosing the same reference units as in table 2.

For models a and b (Jovian planet) a linear fit already gives a good description of the angular momentum evolution of the planet, but an exponential fit has also been performed because, on a longer time-scale (a few thousands orbits), the curve showing j as a function of time could resemble that of the c and d models. We are therefore able to analyse the different migration lifetimes through comparable parameters (exponential lifetime or linear constant derivative).

model	a	b	c	d	e	1/b (years)	1/d (years)
18a	62.87	-3.4×10^{-8}	-3.412×10^{-2}	1.059×10^{-5}	2.2×10^{-2}	-2.66×10^4	8.54×10
18b	-1.054×10^{-3}	7.134×10^{-5}	62.84	-3.994×10^{-8}	0.0	1.27×10	-2.27×10^4
18c	138.4	-4.426×10^{-4}	7.672	3.873×10^{-5}	0.0	-2.04	2.34×10
18d	133.1	-4.547×10^{-4}	10.12	1.822×10^{-5}	0.0	-1.99	4.97×10
36a	62.84	-3.02×10^{-8}	1.228×10^{-4}	1.519×10^{-4}	-4.0×10^{-3}	-3.00×10^4	5.96
36b	62.83	-3.209×10^{-8}	1.538×10^{-3}	8.522×10^{-5}	5.0×10^{-3}	-2.82×10^4	1.06×10
36c	77.65	-1.842×10^{-4}	7.86	6.437×10^{-5}	0.0	-4.91	1.41×10
36d	63.92	-2.191×10^{-4}	20.37	7.021×10^{-6}	0.0	-4.13	1.29×10^2
54a	2.84	-1.557×10^{-8}	7.47×10^{-6}	2.087×10^{-4}	-4.0×10^{-3}	-5.81×10^4	4.33
54b	0.1758	-1.734×10^{-5}	62.66	2.504×10^{-8}	2.2×10^{-3}	-5.22×10	3.61×10^4
54c	-	-	-	-	-	-	-
54d	56.29	-4.93×10^{-5}	14.5	3.032×10^{-5}	0.0	-1.84×10	2.98×10
kepl_a	62.83	5.484×10^{-10}	6.264×10^{-5}	8.953×10^{-5}	1.7×10^{-3}	1.65×10^6	1.01×10
kepl_b	62.83	4.825×10^{-10}	1.375×10^{-4}	6.635×10^{-5}	1.65×10^{-3}	1.87×10^6	1.36×10
kepl_c	65.74	-6.256×10^{-7}	-2.903	-1.407×10^{-5}	0.0	-1.45×10^3	-6.43×10
kepl_d	-1.982	1.227×10^{-5}	64.83	3.28×10^{-7}	0.0	7.37×10	2.76×10^3

Table 2. Exponential best-fit parameters for the specific angular momentum time evolution. A rough estimate of migration times is given by the inverse of the two parameters b and d , dimensioned values in *years* are given in 7th and 8th columns, calculated under the hypothesis of $1 M_{\odot}$ star with a radius of $\sim 2 R_{\odot}$.

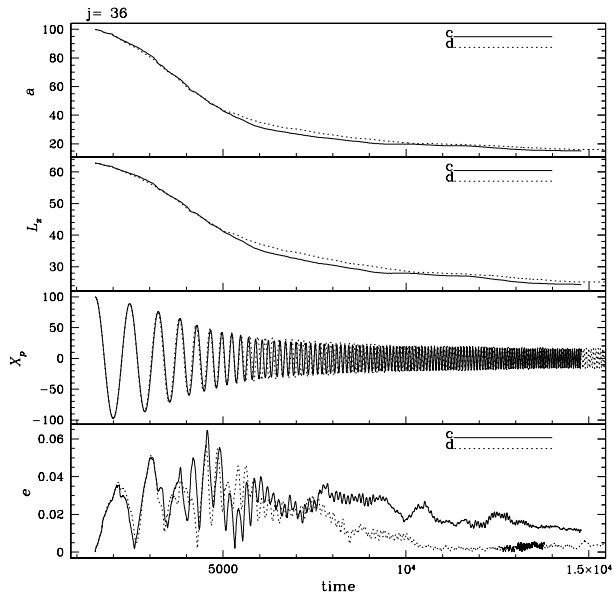


Figure 5. Orbital parameters evolution for models 36c and 36d. See fig. 2 caption for description.

For some of c and d models, the behaviour is initially linear and it becomes more exponential once the protoplanet reaches a position closer to the star. In these cases, the linear fit has been done for a limited time interval during which the evolution does not show a significant migration rate variation. A peculiar case is the 54c model where an initial linear behaviour with negative derivative is followed by a nearly complete migration stop. The exponential fit has not been evaluated for this model.

Propagation of waves coming from the central zone of the disc has been observed, at least for the $j = 18$ and $j = 36$ models. Some snapshots showing this phenomenon are plotted in figures 14 and 15. The same is not clearly observed

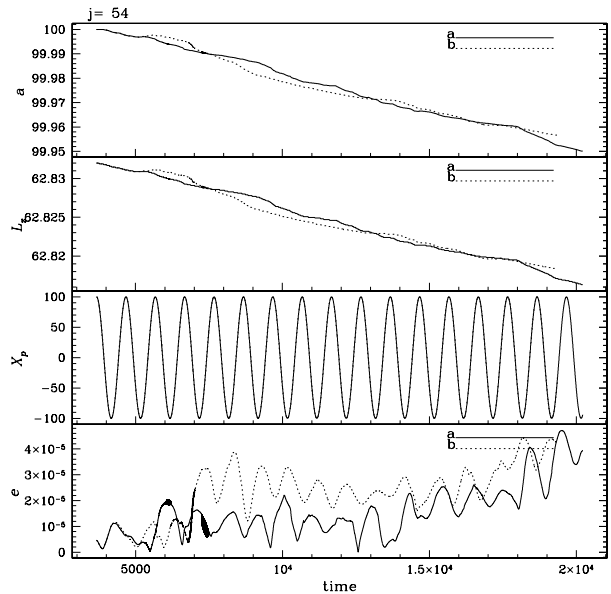


Figure 6. Orbital parameters evolution for models 54a and 54b. See fig. 2 caption for description.

in the other models, the cause being probably the high angular momentum of particles. A strong sub-Keplerian condition for injected particles makes them rapidly fall towards the centrifugal barrier, and the subsequent bouncing-back could be at the origin of these waves. Details on this propagation of shock waves in systems with a central accreting object was described by Lanzafame et al. (2008) and references therein. A proper combination of sub-Keplerian gas flow and viscosity parameter values can create a complex shock structure with nearly periodical radial motions of the shock front. Periods of quiet piling up of particles near and below the centrifugal barrier are followed by the development of a shock front propagating outwards. In low or no

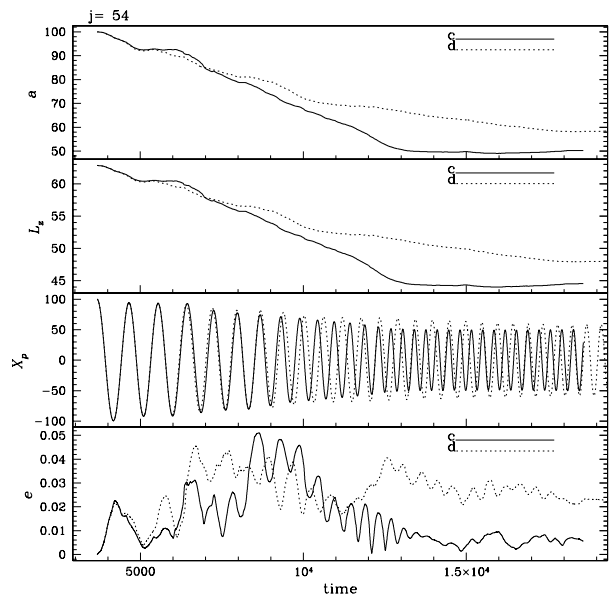


Figure 7. Orbital parameters evolution for models 54c and 54d. See fig. 2 caption for description.

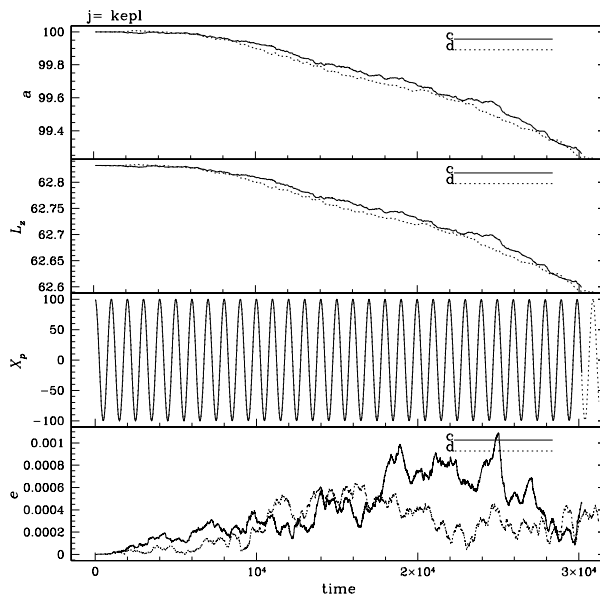


Figure 9. Orbital parameters evolution for the Keplerian models and the Earth-like planet. See fig. 2 caption for description.

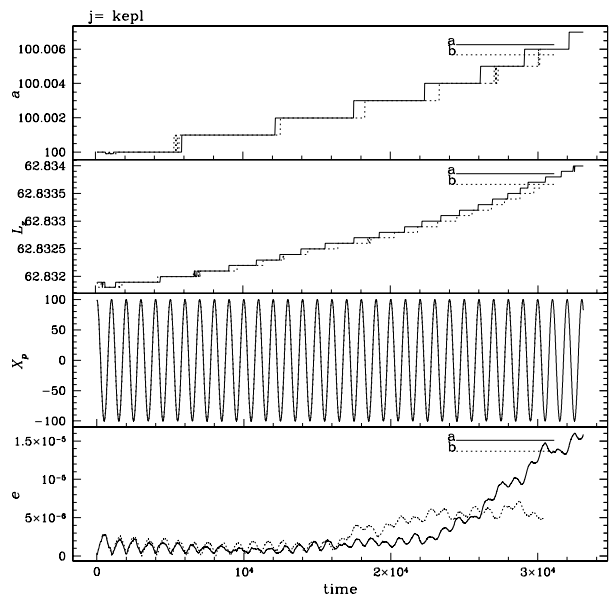


Figure 8. Orbital parameters evolution for the Keplerian models and the Jovian planet. See fig. 2 caption for description.

viscosity regimes, the position of the shock front is generally closer to the central accreting object.

4 DISCUSSION

In a standard disc model, the relation connecting the disc thickness H , the disc radius r is: $H/r = c_s/v_{kepl}$, where c_s is the sound velocity and v_{kepl} is the Keplerian velocity at the disc outer edge. Such relation correlates the disc

model	a	b	τ (adim)	τ (years)
18a	-2.555×10^{-6}	62.838	2.46×10^7	2.23×10^4
18b	-2.717×10^{-6}	62.84	2.31×10^7	2.09×10^4
18c	-1.48685×10^{-2}	93.2653	4.23×10^3	3.83
18d	-141492×10^{-2}	90.8171	4.44×10^3	4.02
36a	-1.762×10^{-6}	62.836	3.57×10^7	3.23×10^4
36b	-1.638×10^{-6}	62.836	3.84×10^7	3.47×10^4
36c	-6.49898×10^{-3}	74.9447	9.67×10^3	8.75
36d	-6.37015×10^{-3}	74.307	9.86×10^3	8.92
54a	-9.533×10^{-7}	62.836	6.59×10^7	5.96×10^4
54b	-9.36912×10^{-7}	62.8356	6.71×10^7	6.07×10^4
54c	-1.90167×10^{-3}	70.8222	3.30×10^4	29.9
54d	-1.42529×10^{-3}	68.0032	4.41×10^4	39.9

Table 3. Linear best-fit parameters for the specific angular momentum time evolution. For some cases, the linear fit is calculated over a limited time interval, during which the angular momentum evolution is linear. The linear fits are not present for the Keplerian models since there is no time interval during which the evolution of the angular momentum is linear. Migration times estimated with the formula l_z/l_z are reported in the last two columns: in the fourth column the dimensionless time is reported, while in the last column the same time is converted in *years* by choosing $1 M_\odot$ and $2 R_\odot$ as physical reference units.

geometry to a tight Keplerian kinematic condition. In our Keplerian disc model, the velocity of particles at the injectors positions is $v_{kepl} = 0.55$ in the units specified in section 2.1, $c_s = 0.05$ being the sound speed, so that we obtain $H/r \simeq 0.05/0.55 \sim 0.09$. Generally this evaluation applies to a thin disc, where the hypothesis of vertical hydrostatic equilibrium is taken into account (Terquem et al. 2000). If this relation is translated also to sub-Keplerian modelling, it would give $H/r \simeq 0.12, 0.18, 0.36$ for $j = 54, 36, 18$ respectively. However, although these results could give some indication, at least as a rough evaluation, these disc spreads are not strictly correct whenever turbulence and sub-Keplerian

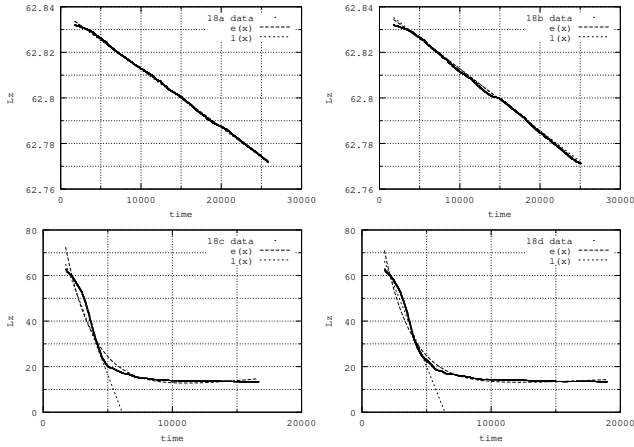


Figure 10. Data and exponential best-fit for angular momentum in $j = 18$ models

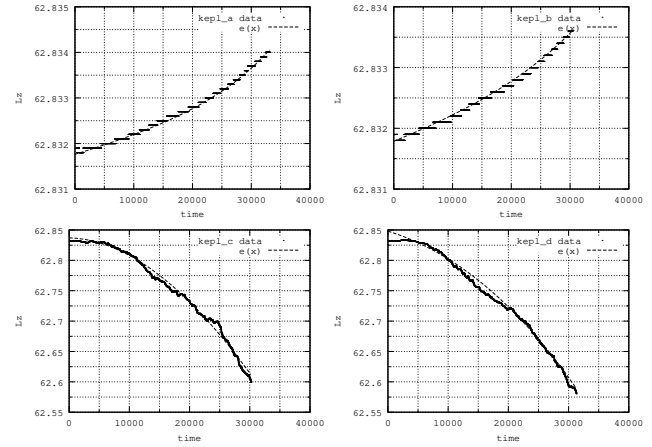


Figure 13. Data and exponential best-fit for angular momentum in Keplerian models

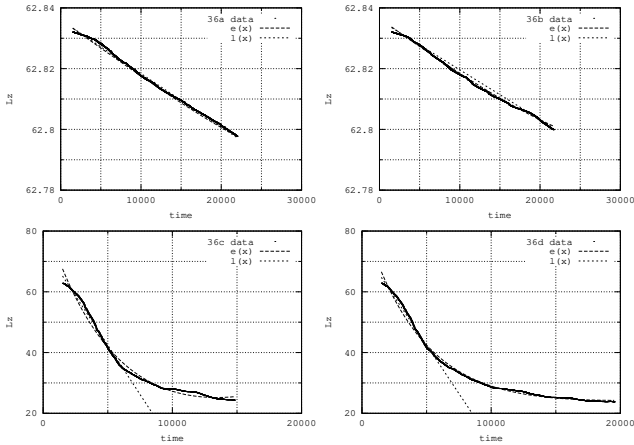


Figure 11. Data and exponential best-fit for angular momentum in $j = 36$ models

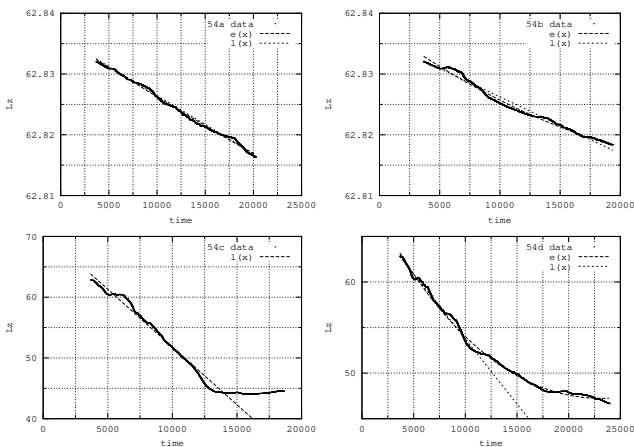


Figure 12. Data and exponential best-fit for angular momentum in $j = 54$ models

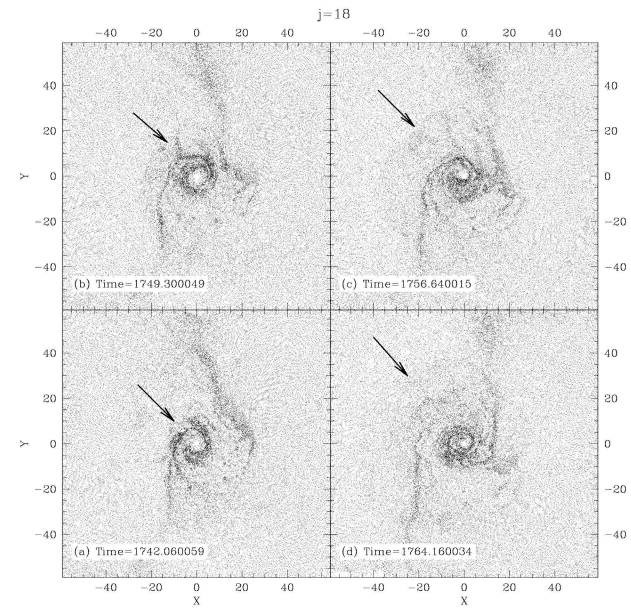


Figure 14. Wave propagation in the $j = 18$ accretion disc. The four snapshots are ordered according to increasing time, starting from the bottom-left square in clock-wise order. The arrows indicate the position of the shock front.

conditions are taken into account. The results of this work deal with protoplanet migration in a protoplanetary accretion disc around a pre-main sequence star, according to the realistic hypothesis that the accretion process is not strictly Keplerian. The Keplerian constraint is usually sustainable on the grounds of the absence of pressure and other forces. Pressure forces and interaction with the protoplanet break almost immediately any initially Keplerian distribution of the gas particle velocity. This is shown in fig. 17 where the radial velocity distribution as a function of radial distance is plotted for one of our initially Keplerian models (*kepl_a*). Initially the radial velocity is zero for all particles. After a half planet orbit the whole distribution of positive and negative radial velocities comes out. Super-Keplerian flows will tend to expel particles outside of the disc area, but sub-

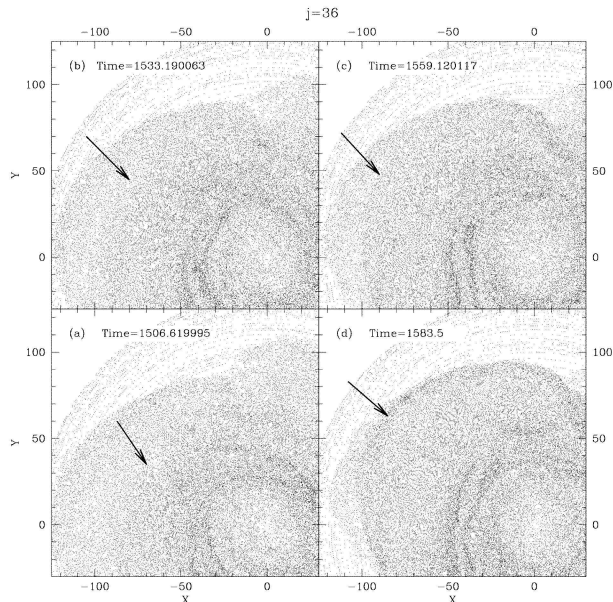


Figure 15. Wave propagation in the $j = 36$ accretion disc. The four snapshots are ordered according to increasing time, starting from the bottom-left square in clock-wise order. The arrows indicate the position of the shock front.

Keplerian flows will develop, both near the planet region and at the inner edge of the disc. Several sub-Keplerian candidates are here taken into account, together with a full treatment of the pressure forces role.

Our models are technically considered as physically inviscid. Artificial viscosity (Monaghan 1992) is introduced in our models to resolve shocks numerically, to avoid spurious heating and to handle fluid discontinuities. Artificial viscosity vanishes when the limit value of the particle interpolation domain goes to zero. The artificial viscosity is necessarily included, and the linear α_{SPH} and quadratic β_{SPH} artificial viscosity terms (usually ~ 1 and sometimes, in some specific cases, < 1) are chosen to be 1 and 2, respectively. Meglicki et al. (1993); Drimmell (1996); Murray (1996); Okazaki et al. (2002) demonstrated that the linear component of the artificial viscosity, in the continuum limit, yields a viscous shear force. Murray (1996) and Okazaki et al. (2002) explicitly formulated such an artificial viscosity contribution in momentum and energy equations, founding an analogy between the shear viscosity generated by the linear artificial viscosity term and the well-known Shakura & Sunyaev (1973) shear viscosity in the continuum limit. In the SPH method, the quadratic (β_{SPH} , von Neumann-Richtmyer like viscosity) artificial viscosity term is used in order to handle structures. An analytical formulation, describing the numerical artificial viscosity coefficient, is reported in Molteni et al. (1991): $\nu_{num} = c_s h$, where c_s is the sound velocity. Therefore, in our modelling, any radial transport process is due to the role of the artificial viscosity. Concerning the difference between the faster migration in our sub-Keplerian models and slower migration in Keplerian ones, we can notice that: in sub-Keplerian models the most important contribution to downward migration seems to come from momentum transfer between the gas particles

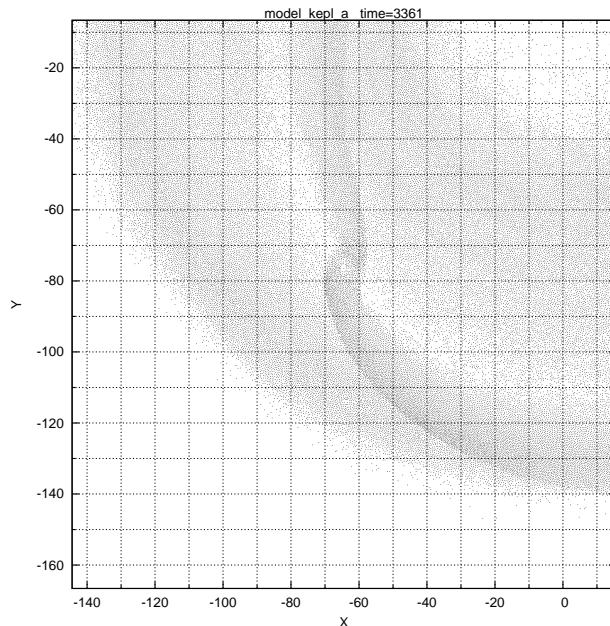


Figure 16. Distribution of the gas particles around a Jupiter-like protoplanet in the initially Keplerian accretion disc. This snapshot corresponds to a $\Delta t \sim 3300$ after the artificial formation of a purely Keplerian velocity distribution, which corresponds to a bit more than 3 orbits of the protoplanet.

and the protoplanet; the sub-Keplerian j_z value induces an average decrease of planet l_z , until the accretion disc centrifugal barrier is reached; an initially Keplerian distribution of gas particles velocities, like in our Keplerian models, makes this effect less important, particularly with the Jovian planet. Models *kepl_a* and *kepl_b* show in fact a slow outward migration, despite the opening of a density gap. This result is different from classical views on the subject, which connect the opening of a density gap to a viscosity driven downward migration (type II migration), but without physical viscosity (our models) the result can be different. Some people (Papaloizou et al. 2006) suggest a type III migration mechanism, where the main migration “engine” is provided by material flowing through the co-orbital region. This material would change orbit (and angular momentum) while passing through the co-orbital, exerting a torque onto the protoplanet. this torque can be evaluated through momentum conservation. This effect might actually be present in our models, but it’s not the main mechanism, at least in our sub-Keplerian models. In our case, momentum conservation is directly applied to correct the protoplanet kinematics when disc particles are captured by the planet. A rough estimate of the specific angular momentum change due to the capture of one disc particle can be done as follows: let l , j , M and m be the specific angular momentum and mass of the protoplanet and of the gas particle respectively; angular momentum conservation after particle capture leads to $\Delta l = m/(M+m)(j-l) \sim m/M(j-l)$ for $m/M \ll 1$; in our case (planet at an initial distance of 100 in a circular Keplerian orbit) $l_{initial} = 62.8$; referring to our 36c model we have $m/M = 10^{-4}$ and $j = 36$, so that after a single capture $\Delta l \sim -2.7 \times 10^{-3}$. About 10^5 particles are captured during our simulation in model 36c before the angular momentum

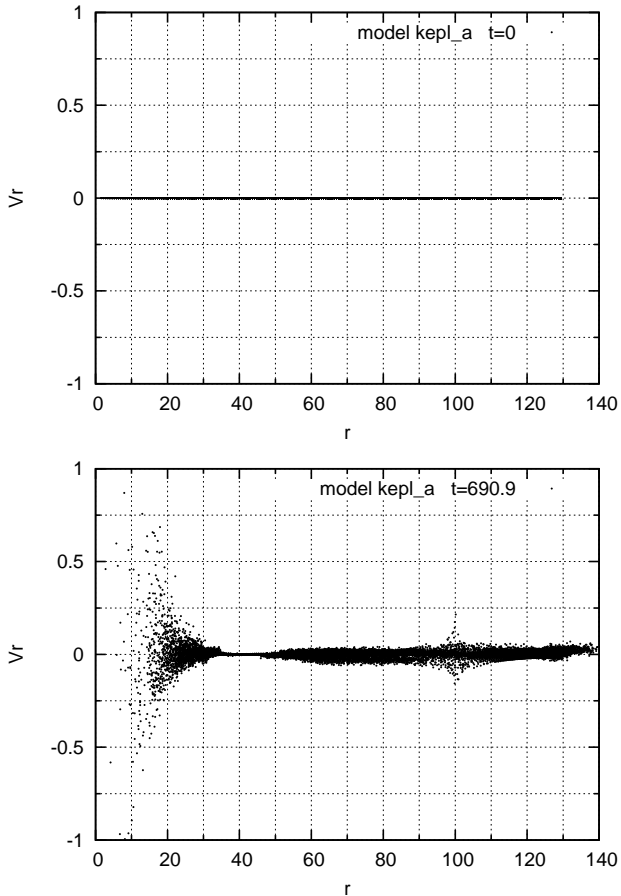


Figure 17. Radial velocity distribution as a function of radial distance for the *kepl_a* model. The graph on top shows the initial totally Keplerian condition, the bottom graph shows the distribution obtained after a time of about ~ 700 (one orbital period is 1000).

is reduced to about one half of the initial value (not all of them will have preserved the $j = 36$ before capture), so that this capture mechanism is perfectly able to account for our rapid migration.

In our Keplerian models particle captures can both increase or decrease the protoplanet angular momentum, and a flow of particles through the co-orbital region is visible (figure 16), so type III mechanism might play a role. Notice however that the above specified flowing particles are moving towards smaller orbits, so they are mostly losing angular momentum. This might actually be the reason for our slowly increasing angular momentum of the protoplanet in *kepl_a, b* models. But, being particle captures present in all our models, we cannot have pure type III migration anyway.

The results also lead our attention to the secondary role of the presence of a “pseudo-atmosphere” surrounding the protoplanets with the aim to discover whether such cumulative role could be also relevant.

The impact of the eventual presence of a pseudo-atmosphere in the protoplanets is visible in some models, particularly those with the less massive protoplanets (look at the difference between models 54c and 54d), but never appears crucial in determining the main results. The slightly faster migration rate shown by models without the pseudo-atmosphere

was actually expected, because the pseudo-atmosphere adds a repulsive pressure interaction between the protoplanet and the gas, that should hinder gas particle capture by the protoplanet. Since part of the migration effect in our models is due to momentum transfer between the infalling particles and the protoplanets when the former are captured, a lower capture rate might bring a lower migration rate.

Particularly interesting is the result reported by the *c, d* models, where the radial migration breaks down close to $\sim 15; 20; 45$ stellar radii, for $j = 18; 36; 54$ respectively. We believe that this effect is mainly due to the interaction of the protoplanet with the propagation of outward gas waves coming from inner zones (figures 14-15), where the centrifugal barrier is located in our sub-Keplerian models. These results show that, despite the sub-Keplerian and more realistic conditions, planetary migration could even halt. Subsequent disc extinction could freeze the protoplanet orbital parameters. Of course, due to a much higher inertia, Jovian planets evolve much more slowly.

An analytical expression giving us an idea of the protoplanet evolution, as a function of the model initial conditions, is expressed by the specific angular momentum fit equations 1-2 and by their temporal first derivatives.

Even if it is not the main topic of this paper, let’s draw some comments on eccentricity behaviour shown in the bottom rectangles of figures 2-9. For Jupiter-like planets the orbits remain almost circular, with values around 10^{-5} , while for Earth-like planets some eccentricity enhancing effect is visible in sub-keplerian models, but the behaviour is quite complex and a more stable value is obtained in late migration phases, with values in the 0.01 – 0.02 range.

For a comparison with other results we refer to the study performed by Schäfer et al. (2004) since they used SPH to simulate accretion disc hydrodynamics, even if some differences have to be remarked: first, they use a different numerical method to avoid particle mutual penetration, since they rely on XSPH with a bulk viscosity contribution to the viscous stress tensor; second, they simulate physical viscous discs according to Shakura & Sunyaev (1973) prescription whilst our discs are inviscid; third, they use an isothermal equation of state whilst we rely on a classical ideal gas equation with variable thermal energy per unit mass; fourth, their initial velocity distribution is Keplerian. They estimate a decrease of the planet distance from the the star of about 1 AU (from 5.2 AU to 4.1 AU) in about 30000 years for a Jovian planet, which brings to a rate of $Da/Dt \sim 3.3 \times 10^{-5}$ AU/y. They also conclude that migration is braked by disc mass loss, which means a lowering of the disc density and of the gravitational interaction.

Inserting in our dimensionless model the following reference physical units: central star mass $M_0 = 1M_\odot$; stellar radius from typical T-Tauri stars (Bertout 1989) $R_0 \sim 2R_\odot$; the basic unit for time is $T_0 \sim 2.8 \times 10^4$ s. Our sub-Keplerian models with $j = 18; 36; 54$ give then migration rates of $Da/Dt \sim 8 \times 10^{-5}; 5.3 \times 10^{-5}; 3.4 \times 10^{-5}$ AU/y respectively. We notice that our $j = 54$ (the less sub-Keplerian model) migration rate is similar to the average migration rate obtained by Schäfer et al. (2004), even if our starting distance is about 1 AU with the above specified choices for physical units. More important, the braking effect is due, in our simulations, to a completely different mechanism based on turbulence, outward propagation of bouncing waves and changing

of the average momentum transferred to the planet during gas particle captures, and we do not observe a significant lowering of the disc density.

ACKNOWLEDGEMENTS

The computational resources used to develop this work were provided by the COMETA consortium (<http://www.consorzio-cometa.it>), through the PI2S2 project (<http://www.pi2s2.it>). A special thank goes to Alessandro Grillo for useful help and technical support in using the COMETA computational GRID resources.

REFERENCES

- Artymowicz P., 2004, ASP Conference Series, Vol. 324, pag. 39
- Bertout C., 1989, *Annu. Rev. Astron. Astrophys.*, 1989, 27, 351
- Chakrabarti S.K., Molteni D., 1993, *ApJ*, 417, 671
- Cresswell P., Nelson R. P., 2006, *A&A*, 450, 833
- D'Angelo G., Henning T., Kley W., 2002, *A&A*, 385, 647
- D'Angelo G., Kley W., Henning T., 2003, *ApJ*, 586, 540
- D'Angelo G., Lubow S.H., Bate M.R., 2006, *ApJ*, 652, 1698
- Del Popolo A., Ercan N., Yesilyurt I.S., 2005, *A&A*, 436, 363
- de Val-Borro M., Edgar R.G., Artymowicz P., Cieliegielag P., Cresswell P., D'Angelo G., Delgado-Donate E. J., Dirksen G., Fromang S., Gawryszczak A., Klahr H., Kley W., Lyra W., Masset F., Mellema G., Nelson R.P., Paardekooper S.-J., Peplinski A., Pierens A., Plewa T., Rice K., Schäfer C. and Speith R., 2006, *MNRAS*, 270, 529
- Drimmell R., 1996, *MNRAS*, 282, 982
- Gullbring E., Hartmann L., Briceno C., Calvet N., *ApJ*, 492,323
- Goldreich P., Tremaine S., 1979, *ApJ*, 233, 857
- Goldreich P., Tremaine S., 1980, *ApJ*, 241, 425
- Hartigan P., Edwards S., Ghandour L., 1995, *ApJ*, 452, 736
- Hartmann L., 2000, ASP Conference Series, Vol. 219, pag. 95
- Kley W., 2000, ASP Conference Series, Vol. 219, pag. 69
- Lanzafame G., Molteni D., Chakrabarti S.K., 1998, *MNRAS*, 299, 799
- Lanzafame G., Cassaro P., Schilliró F., Costa V., Belvedere G., Zappalà R. A., 2008, *A&A*,482, 473
- Lin D. N. C., Papaloizou J., 1984, *ApJ*, 285, 818
- Lin D. N. C., Papaloizou J., 1986, *ApJ*, 307, 395
- Lin D. N. C., Papaloizou J., 1986, *ApJ*, 309, 846
- Meglicki Z., Wickramasinghe D., Bicknell G. V., 1993, *MNRAS*, 264, 691
- Molteni D., Belvedere G., Lanzafame G., 1991, *MNRAS*, 249, 748
- Molteni D., Lanzafame G., Chakrabarti S.K., 1994, *ApJ*, 425, 161
- Monaghan, J.J., 1992, *Annu. Rev. A&A*, 30, 543
- Murray J. R., 1996, *MNRAS*, 279, 402
- Okazaki A. T., Bate M. R., Ogilvie G. I., Pringle J. E., 2002, *MNRAS*, 337, 967
- Papaloizou J. C. B., Nelson R. P., Kley W., Masset F. S., Artymowicz P., 2006, *Protostars and Planets V*
- Paardekooper S.-J., Mellema G., 2004, *A&A*, 425, L9
- Perryman M.A.C., 2000, *Rep. Prog. Phys.*, 63, 1209
- Schäfer C., Speith R., Hipp M., Kley W., 2004, *A&A*, 418, 325
- Shakura N. I., Sunyaev R. A., 1973, *A&A*, 24, 337
- Sollins P. K., Ho P. T. P., 2005, *ApJ*, 630, 987
- Tanaka H. Takeuchi T., Ward W. R., 2002, *ApJ*, 565, 1257
- Terquem C., Papaloizou J. C. B., Nelson R. P., 2000, ASP Conference Series, Vol. 219, pag. 19
- Udry S., Santos N.C., 2007, *Annu. Rev. Astron. Astrophys.*, 45, 397
- Ulrich R. K., 1976, *ApJ*, 219, 377
- Ward W.R., 1997, *ApJ*, 482, L211
- Xu J., Stone J. M., *ApJ*, 454,172